Macromolecules 1998, *31*, 8448–8454

Long-Chain Branched Polyethene Polymerized by Metallocene Catalysts Et[Ind]$_2$ZrCl$_2$/MAO† and Et[IndH$_4$]$_2$ZrCl$_2$/MAO‡

Anneli Malmberg, Esa Kokko, Petri Lehmus, Barbro Löfgren, and Jukka V. Seppälä*

Helsinki University of Technology, Department of Chemical Technology, P.O. Box 6100, FIN-02015 HUT, Finland

Received April 3, 1998; Revised Manuscript Received September 8, 1998

ABSTRACT: Ethene homopolymers and ethene copolymers with 1-hexene were prepared by Et[Ind]$_2$ZrCl$_2$/MAO and Et[IndH$_4$]$_2$ZrCl$_2$/MAO catalyst systems in slurry polymerizations. The melt behavior of the polymers was studied with small amplitude dynamic rheological measurements. The low-frequency complex viscosity of the polymers was higher than expected on the basis of their GPC molecular weights. Furthermore, the polymers exhibited elevated activation energy for flow. The polymers catalyzed by Et[Ind]$_2$ZrCl$_2$/MAO had an Arrhenius-type flow activation energy of 50–60 kJ/mol, and those catalyzed by Et[IndH$_4$]$_2$ZrCl$_2$/MAO a somewhat lower value of 40 kJ/mol. Branching could be detected by ^{13}C NMR in homopolyethene samples polymerized by Et[Ind]$_2$ZrCl$_2$/MAO. We suggest that these properties are due to long-chain branching that occurs via in situ incorporation of vinyl-terminated polyethene macromonomers. With Et[Ind]$_2$ZrCl$_2$/MAO the polymerization parameters affecting the rheological behavior most were ethene partial pressure and comonomer concentration, whereas with Et[IndH$_4$]$_2$ZrCl$_2$/MAO the major factor was the amount of hydrogen.

Introduction

Metallocene and single site catalysts enable the production of controlled structure ethene homo- and copolymers, and some reports in the patent literature describe their successful application in the production of long-chain branched polyethene.[1] Although controlled structure is not achieved in conventional low-density polyethene, it continues to be widely used owing to its good rheological properties. These properties are due to the long-chain branches that are formed via a free radical mechanism at high pressures. Long chain branching does not occur, or is only minimal, when Ziegler–Natta catalysts are used in low-pressure polymerizations.

Only a few publications have dealt with the long-chain branching produced by metallocene and single site catalysts. Lai et al.[1b] report the production of long-chain branched polyethene with [CpSiMe$_2$N(t-Bu)]TiCl$_2$, a "constrained geometry catalyst". Shiono et al.[2] were able to incorporate polypropene macromonomers into the polyethene chain with various metallocene catalysts and, according to Carella,[3] Vega et al.[4] probably obtained long-chain branched polyethenes with Cp$_2$ZrCl$_2$. In addition, Howard et al.[1c] have reported the formation of long-chain branched polyethene in gas-phase polymerization where Et[Ind]$_2$ZrCl$_2$ served as the catalyst.

In the copolymerization of vinyl-terminated polyethene macromonomers with ethene, the extent of the long-chain branching depends mainly on the catalyst system[5] and the conditions used in polymerization.[6] The role of the catalyst is 2-fold. First, the catalyst must be able to produce, selectively, vinyl-terminated chains. These vinyl-terminated chains can be considered as macromonomers. Second, the catalyst must be able to effectively incorporate these macromonomers into the growing polyethene chain.[5]

The polymerization conditions are also important. The main factors are high polymer concentration and low monomer (ethene) concentration.[6] The end group selectivity and/or the copolymerization tendency may also be influenced by the polymerization temperature, reaction medium, and comonomer and hydrogen concentrations.

In this work, we studied the rheological properties of polyethenes and copolymers of ethene and 1-hexene polymerized by Et[Ind]$_2$ZrCl$_2$/MAO (Cat 1) and Et[IndH$_4$]$_2$ZrCl$_2$/MAO (Cat 2) catalyst systems and found that they differed from those of linear polyethenes. Long chain branching was detected by ^{13}C NMR in the Et[Ind]$_2$ZrCl$_2$/MAO-polymerized homopolyethene sample. We suggest that these properties are due to the long-chain branching that occurs via in situ incorporation of vinyl-terminated polyethene macromonomers.

Experimental Section

Polymerization and Characterization. The polymerizations were run in either pentane (series A and C) or toluene (series B and D) in a laboratory-scale slurry reactor. The catalysts were obtained from commercial sources (Witco), as was the 10 wt % methylaluminoxane (MAO) in toluene that was used as cocatalyst. During the polymerization, purified polymerization-grade ethene was fed continuously to maintain the desired ethene partial pressure, but the 1-hexene (Aldrich) and hydrogen were fed batchwise before introduction of the catalyst.

The apparent molecular weights (M_w and M_n) and molecular weight distribution (MWD) were determined on a Waters 150C high-temperature GPC equipped with a refractometer detector. The GPC was calibrated with narrow MWD polystyrene standards that covered the molecular weight region from 10^3 to 10^7. In addition to this, well-characterized polyethene samples were used as internal standards. The samples were dissolved in trichlorobenzene and the measurement was carried out at 140 °C. The intrinsic viscosities were deter-

† *rac*-Ethenebis(indenyl)zirconiumdichloride/methylaluminoxane.

‡ *rac*-Ethenebis(4,5,6,7-tetrahydroindenyl)zirconiumdichloride/methylaluminoxane.

10.1021/ma980522n CCC: $15.00
Published on Web 11/11/1998

mined in decahydronaphthalene at 135 °C using Schott-Gerâte AVS 400 equipment.

The comonomer content was characterized by using FT-IR and ^{13}C NMR spectroscopy. IR analysis was also used to determine the double bond content of the polymers using the method of Haslam et al.[7a] The samples for IR analysis were melt pressed at 190 °C to 0.5 mm thick plates. The IR spectra were recorded using Nicolet Magna FT-IR equipment. ^{13}C NMR spectra were recorded on a Varian XL-300 NMR spectrometer operating at 75 MHz at 125 °C. The pulse angle was 60°, acquisition time 1.8 s and pulse delay 6.0 s. The number of transients was at least 1400. The carbon signals were assigned according to Randall.[7b]

The samples were stabilized for the rheological measurements with 1500 ppm Irganox B 225 FF or 2000 ppm Irganox B 215 antioxidant. After stabilization, the samples were melt pressed at 190 °C into 1 mm thick plates using a Fontijne TP 400 table press.

The rheological measurements were carried out on a Rheometric Scientific stress controlled dynamic rheometer SR-500. All the measurements were carried out within the linear viscoelasticity region, which was ensured by a stress sweep. Frequency sweeps for the polymers were carried out under nitrogen at 170, 190, and 210 °C using a 25 mm plate−plate geometry. The angular frequency was from 0.01 to 100 rad/s, and the sample gap was 1 mm. Rheometrics RSI Orchestrator software was used to shift the moduli curves along the frequency axis to construct the master curves and to determine the shift factor a_T.

Thermal Stability. The thermal stability of the samples during the rheological testing was checked by repeating one low-frequency measurement point after the primary frequency sweep. In no sample was the change in storage modulus G' during the frequency sweep greater than 5%. The thermal stability of selected polymers, representing both catalysts, was also studied in a separate time sweep, where the polymers gave a stable G' signal for at least 90 min at 190 °C. In addition, some samples were analyzed by FT-IR after the rheological analysis. Changes in the double bond pattern were within the range of test reproducibility.

Rheology Reference Samples. Ref-1 was a high molecular weight homopolyethene sample polymerized using (n-butCp)$_2$ZrCl$_2$/MAO catalyst. A flow activation energy of 26 kJ/mol was obtained for this polymer. Ref-2 was a conventional Ziegler−Natta catalyzed film-grade linear low-density polyethene, with few or no long-chain branches, yielding 33 kJ/mol for flow activation energy. Ref-3 was an extrusion coating grade PE-LD with broad molecular weight distribution and a flow activation energy of 55 kJ/mol, typical for low-density polyethene.

Results and Discussion

Linear Viscoelastic Behavior. Figure 1 shows the frequency dependence of the complex viscosity of selected polymer samples of both catalysts at 190 °C. Inspection of the low-frequency complex viscosities in Figure 1 in comparison with the intrinsic viscosities and GPC-measured molecular weights (Tables 1 and 2) reveals a discrepancy. In particular, the complex viscosities of the polymers produced with Cat 1 are higher, and the frequency dependency is very different from what one would expect for a linear polymer on the basis of the GPC-measured molecular weight and rather narrow MWD.

Reference materials Ref-1 and Ref-2 are narrow molecular weight distribution polyethenes, with M_w 380 000, MWD 2.1 and M_w 100 000, MWD 3.8, respectively. GPC analysis gave a M_w of 153 000, MWD 3.6 for polymer B2, yet it has a higher complex viscosity at low frequencies than the high M_w polymer Ref-1. The shear thinning behavior of the complex viscosity of polymer B2 is sharp. Polymer A5, also polymerized with Cat 1, shows similar sharp shear thinning. Furthermore, A5 has a considerably higher complex viscosity at the lowest frequency than do the Cat 2 polymers D1 and C3, although the polymers exhibited similar GPC-measured molecular weights and molecular weight distributions.

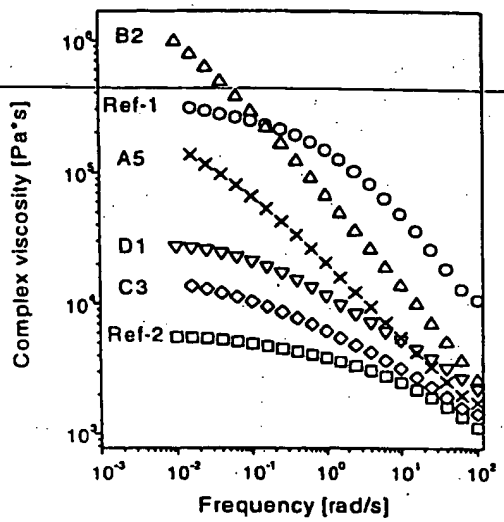

Figure 1. Frequency dependence of the complex viscosity of selected samples at 190 °C (463 K). Samples A5, M_w 115 000, MWD 2.8 and B2, M_w 153 000, MWD 3.6, polymerized with Cat 1. Sample C3, M_w 117 000, MWD 3.6 and D1, M_w 114 000, MWD 2.2 polymerized with Cat 2. Reference material Ref-1, M_w 380 000, MWD 2.1 and Ref-2, M_w 100 000, MWD 3.8. The molecular weights are RI-detector measured GPC values.

The linear viscoelastic properties of the polymer melt are specifically governed by the high molecular weight side of the molecular weight distribution, and by the long-chain branching.[8,9] GPC, on the other hand, inherently lacks sensitivity for small differences in the high molecular weight tail of the molecular weight distribution.[10,11] The contradiction between the observed rheological behavior and the GPC-measured molecular weights and MWDs suggests the presence of at least trace amounts of material with very long relaxation times in the polymers.

Figure 2 presents the frequency dependence of the dynamic moduli at 190 °C. Polymers A5 and B2 were produced with Cat 1, and polymer C3 with Cat 2. GPC analysis revealed very similar molecular weights and MWD for polymers A5 and C3, yet the contribution of the storage modulus G' is clearly greater, and the $G'-G''$ moduli crossover occurs at an earlier point in the A5 polymer. The greatest difference is seen when comparing the frequency dependency of the dynamic moduli of polymers A5 and B2 to the behavior of the high molecular weight, narrow MWD polymer Ref-1. The contribution of the storage modulus G' is much greater in polymers A5 and B2 throughout the frequency scale. The B2 polymer exhibits a very early crossover of the moduli, the storage modulus G' dominating even at very low frequencies. Behavior of this type generally indicates startup of a secondary network structure and is seen, for example, in peroxide cross-linked polyethene in the very early stages of cross-linking.[9,11]

Flow Activation Energy. The observed linear viscoelastic behavior of the polymers produced with Cat

Table 1. Characterization of Polymers[a]

		p(Et), bar	H_2/Zr, mol/mol	comonomer content, wt %	[η][g] (135 °C), dL/g	GPC $10^{-3}M_w$	GPC $10^{-3}M_n$	GPC MWD	FT-IR C=C/1000 C-atoms tv[d]	FT-IR C=C/1000 C-atoms v[e]	FT-IR C=C/1000 C-atoms vd[f]	complex viscosity at 0.02 rad/s and 190 °C, Pa s	TTS E_a, kJ/mol
						Et[Ind]$_2$ZrCl$_2$ (Cat 1)							
A	1	10.0		0.0	1.60	112	35	3.2	0.02	0.62	0.02	58 600	48
A	2	10.0	C6	1.7	1.42	102	38	2.7	0.02	0.55	0.06	68 500	53
A	3	5.0		0.0	1.66	136	41	3.3	0.04	0.47	0.02	251 000	50
A	4	5.0	8300	0.0	1.42	102	27	3.8	0.00	0.41	0.03	132 000	59
A	5	5.0	C6	3.1	1.53	115	41	2.8	0.04	0.49	0.08	136 000	56
A	6	2.5		0.0	1.77	136	46	3.0	0.03	0.41	0.03	nm[b]	
A	7	2.5	C6	5.0	1.24	112	35	3.2	0.07	0.54	0.13	33 400	52
B	1	2.5[c]		0.0		287	78	3.7	0.11	0.14	0.02	nm[b]	
B	2	2.5[c]	C6	7.3		153	42	3.6	0.15	0.12	0.07	710 000	64
B	3	2.5[c]	C6	16.2		78	24	3.3	0.12	0.08	0.21	13 000	59
B	4	1.6	2800	0.0		23	9.6	2.4	0.01	0.31	0.07	nm	
B	5	1.0		0.0		120	46	2.4	0.15	0.20	0.02	nm	
						Et[IndH$_4$]$_2$ZrCl$_2$ (Cat 2)							
C	0	10.0		0.0		nm	nm	nm	0.07	0.03	0.01	nm[b]	
C	1	10.0	8300	0.0	1.62	118	42.8	2.8	0.04	0.06	0.02	34 300	41
C	2	10.0	20000	0.0		48	15.5	3.1	0.00	0.01	0.06	400	32
C	3	10.0	8300 C6	2.5	1.56	117	32	3.6	0.00	0.07	0.06	13 600	38
C	4	5.0	8300 C6	2.9		68	19	3.6	0.01	0.08	0.11	1 300	35
C	5	2.5	2000	0.0	1.19	69	18	3.8	0.00	0.07	0.06	8 500	42
D	1	1.0		0.0		114	51	2.2	0.22	0.11	0.03	26 000	41
D	2	1.0	1300	0.0		60	12	5.0	0.08	0.04	0.07	nm	
D	3	1.0[c]	C6	6.1		140	62	2.3	0.04	0.10	0.12	29 000	39

[a] Polymerizations were run at 80 °C for 60 min, series A and C in pentane, B and D in toluene. Cocatalyst: MAO. Comonomer and hydrogen fed batchwise. nm = not measured. [b] Not measured due to very slow relaxation (very high MW). [c] Polymerization temperature 60 °C. [d] Calculated from *trans*-vinylene absorbance at 965 cm^{-1}. [e] Vinyl absorbance at 908 cm^{-1}. [f] Vinylidene absorbance at 888 cm^{-1}. [g] In decahydronaphthalene.

Table 2. Rheology Reference Materials

sample	type	[η] (135 °C), dL/g	$10^{-3}M_w$	MWD	complex viscosity at 0.02 rad/s and 190 °C, Pa s	TTS E_a, kJ/mol
Ref-1	PE-HD	4.41	380	2.1	307000	26
Ref-2	PE-LLD (ZN)		100	3.8	5500	33
Ref-3	PE-LD		154	9.3	4600	55

1 could also be due to long-chain branching in the polymers. To investigate this view, the Arrhenius type flow activation energies of the polymers were determined. In ethene polymers, the flow activation energy E_a, or temperature coefficient of viscosity, is sensitive to the presence of long branches.[12,13] In the case of linear chains, E_a does not depend on molecular weight.[14] For branched polymer, the increase of E_a above the value for linear polyethenes is directly proportional to branch length, while in blends of linear and branched material, it is proportional to the volume fraction of the branched polymer.[15]

Flow activation energy values of around 27 kJ/mol are usually reported for linear PE-HD type polyethene.[14,16] We obtained 26 kJ/mol for the homopolyethene sample Ref-1, which thus appears to be very linear. A value of E_a of 33 kJ/mol was calculated for the PE-LLD sample Ref-2 and 55 kJ/mol for the PE-LD sample Ref-3. All these values are in accordance with other studies.[14,17] For single site catalyzed, controlled long-chain branched polyethenes,[17] E_a values ranging from 33 to 39 kJ/mol, based on data from capillary rheometry, are reported. Values from 34 (low M_w) to 38 kJ/mol (high M_w) are reported for ethene polymers polymerized with Cp_2ZrCl_2/MAO catalyst.[4] These polymers also exhibit the contradiction between low-frequency complex viscosity and GPC-measured molecular weight. As noted by Carella,[3] these polymers appear to be long-chain branched, although long-chain branching was not seen in ^{13}C NMR studies.

Interestingly, we obtained high values of flow activation energy, 40 kJ/mol, for the experimental polymers prepared with Cat 2 and values comparable to those of PE-LD, over 50 kJ/mol, for polymers produced with Cat 1.

The observed rheological behavior might be explained by long-chain branching formed by the formation and in situ incorporation of vinyl-terminated macromonomers into a growing chain. Another explanation could be chain extension or cross-linking of the chains due to thermal degradation during sample preparation. Polymers bearing a high content of unsaturation are prone to chain extension as the main mechanism of thermo-oxidative degradation. This chain enlargement is readily seen in the dynamic melt rheology, but it also causes changes in the double bond pattern of the polymer.[18,19] As noted in the Experimental Section, thermal stability of the experimental polymers was studied and found to be good.

^{13}C NMR Measurements. From the rheological measurements, the polymers produced with Cat 1 and Cat 2 appear to be long-chain branched. This conclusion obtains strong support from ^{13}C NMR. Figure 3 shows the ^{13}C NMR spectrum of the homopolyethene sample B5. The end group peaks are located at 14.1, 22.9, and 32.2 ppm. The carbons next to a branch point, the α- and β-carbons, are clearly visible at 34.5 and 27.3 ppm. The tertiary carbon atom of the branch point is seen at 38.1 ppm. According to this analysis, the homopolyethene sample B5 contains branches longer than six carbon atoms. The estimated content of the branches is maximum 0.2 branches per 1000 carbon atoms.

Influence of Polymerization Parameters. The hypothesis of in situ macromonomer incorporation is further supported by our finding that the rheological properties of the polymer can be altered by changing

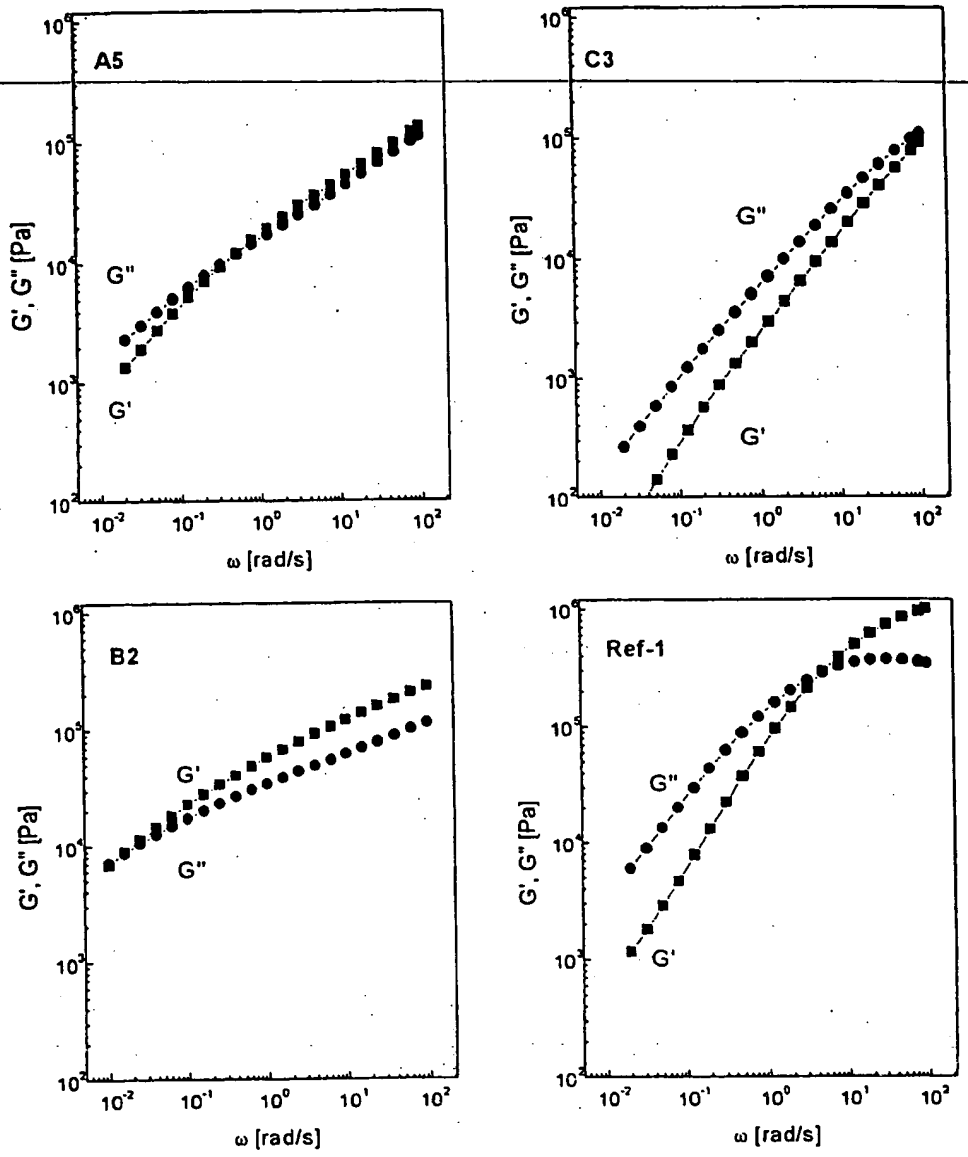

Figure 2. Dynamic moduli as function of measurement frequency at 190 °C (463 K). The molecular weight characteristics as in Figure 1.

the polymerization parameters of monomer pressure and the amounts of comonomer and hydrogen. With Cat 1, the major factors affecting the rheological behavior were ethene partial pressure and comonomer concentration, whereas with Cat 2 the major factor was the amount of hydrogen in the polymerization.

In copolymerization, the higher the ethene concentration the more likely it becomes that ethene is inserted instead of comonomer (or macromonomer), and a more linear polymer is formed. The results of the copolymerization as a function of ethene pressure (samples A2, A5, and A7) showed that when pressure was decreased from 10 to 2.5 bar the amount of 1-hexene incorporated increased from 1.7 wt % to 5.0 wt %. A similar trend is possible in the incorporation of the macromonomers.

In a semibatch slurry reactor, the concentration of macromonomers increases with time, while the concentration of ethene may decrease due to mass transfer limitations. Diffusion limitations also broaden the molecular weight distribution in copolymerizations. However, this cannot explain the rheological behavior observed. With Cat 1, decreasing ethene partial pressure in polymerization increased the low frequency viscosity of the polymer. This can be seen by comparing polymers A1, A3, and A6 polymerized at 10, 5, and 2.5 bar ethene partial pressure but otherwise under identical conditions. The low-frequency viscosity was considerably higher for A3 than for A1 (see Table 1), and A6 could not be rheologically analyzed at all due to extremely slow relaxation, indicating a very high zero shear viscosity. From the GPC-measured molecular weights of the polymers, one would nevertheless have expected almost identical low-frequency viscosities.

The catalysts differed in their response to hydrogen in the polymerization. With Cat 2, both the molecular

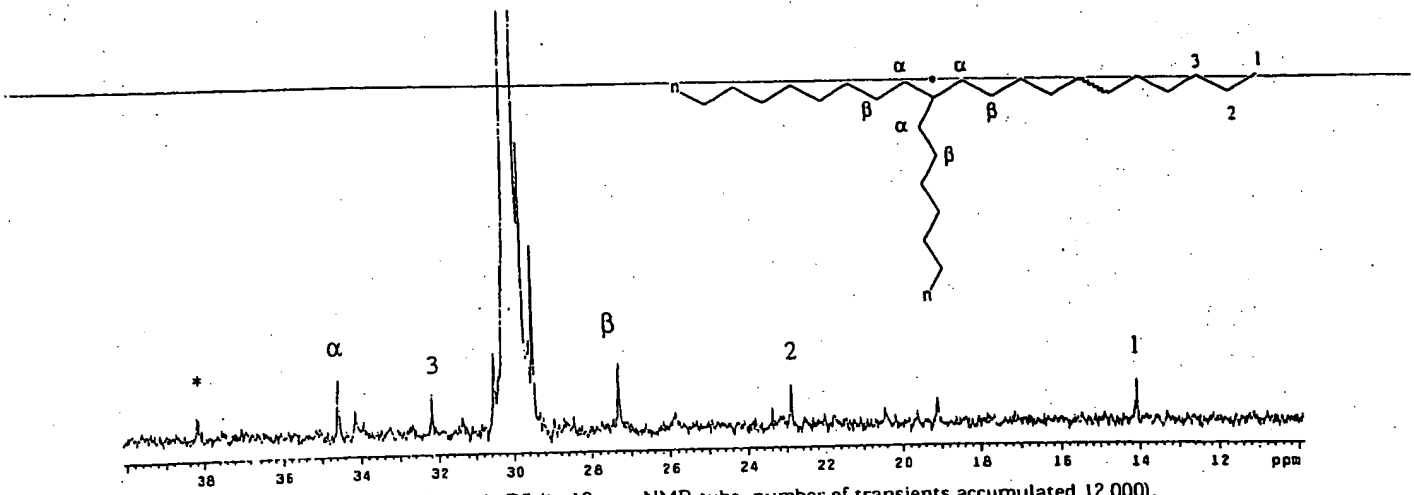

Figure 3. ^{13}C NMR spectrum of sample B5 (in 10 mm NMR tube, number of transients accumulated 12 000).

weight and the flow activation energy were clearly lower (compare polymers C1 and C2) with an increased amount of hydrogen. With Cat 1 (polymers A3 and A4), molecular weight and complex viscosity were decreased, but not the flow activation energy. An increasing content of comonomer in the polymer, with no hydrogen present in the polymerization, seemed to reduce the E_a (polymers B2 and B3).

Double Bond End Group Analysis. Study of the double bond containing end groups of the polymers by FT-IR revealed some interesting differences between the catalysts. The presence of three types of olefinic end groups, transvinyl ($\nu = 965$ cm^{-1}), vinyl ($\nu = 910$ cm^{-1}), and vinylidene ($\nu = 888$ cm^{-1}), was analyzed. Table 1 shows the results of the IR analysis. With metallocene catalysts, the β-H elimination to monomer and β-H elimination to the metal are the most likely termination mechanisms producing vinyl ends.[20] Another possible way in which vinyl terminal groups are formed is the C−H activation or σ-bond metathesis route.[21,22] The more comonomer added, the more likely it is that termination via β-H elimination occurs after insertion of comonomer, which produces vinylidene ends. However, chain termination after insertion of ethene may also be present. The termination after insertion of ethene is seen as a relatively large amount of vinyl groups in the copolymers.

Figure 4 shows the double bond region of the IR spectra of some B and D series polymers. Polyethene produced with Cat 1 (sample B5) contained a larger fraction of vinyl end groups, while Cat 2 (sample D1) tended to produce more transvinyl-terminated polyethene. Cat 2 was also more sensitive to chain transfer agents such as comonomer and hydrogen. More olefinic end groups disappeared from the polymer when hydrogen was introduced with Cat 2 (sample D2), and the same sensitivity was observed when the comonomer was introduced (sample D3). At the same comonomer content, copolymer produced with Cat 1 contained less vinylidene end groups (sample B2), but the extent of the phenomenon may be exaggerated by the different polymerization pressures used in B2 and D3.

As can be seen from Table 1, hydrogen reduced the molecular weight and altered the end group pattern in two ways. First, the number of double bonds per chain was reduced because of chain transfer to hydrogen, and

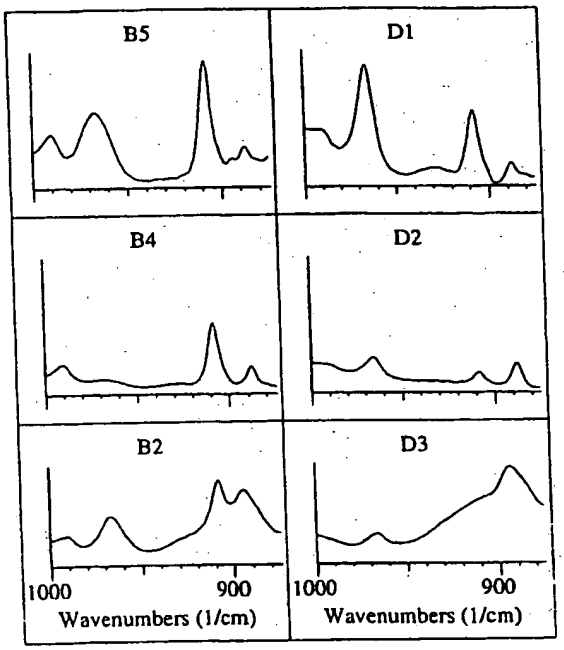

Figure 4. Comparison of the olefinic end groups of Cat 1 and Cat 2 polymers.

second, the transvinyl double bonds disappeared. This behavior, together with the catalyst activating effect of hydrogen, has also been reported by other groups.[23,24] We found that, in the A and C series, the presence of hydrogen had only a minor effect on the polymerization yield. The polymer yield increased with Cat 2 and the greatest yields were obtained when both comonomer and H_2 were present in the polymerization.

Comparison of Catalyst Behavior. Overall, the ligand has a notable influence on the polymerization behavior of the metallocene catalysts. The ligand structure has both steric and electronic effects, but the reasons for the different behavior are not completely understood. In general, hydrogenation of the indenyl ligand of a bridged catalyst increases the molecular weight of the polyethene product while decreasing the polymerization activity. The molecular weight distribu-

tion seems to be slightly broader for the ethene-bridged indenyl ligand catalyst (Cat 1). The hydrogenated indenyl catalyst (Cat 2) is more sensitive to comonomer in the sense that the molecular weight of the copolymer decreases more dramatically with increasing comonomer content. Cat 1 has been found to incorporate the comonomer slightly better than Cat 2.[25-27]

As discussed by Spaleck et al.,[27] there may be several reasons for the different sensitivity of Cat 1 and Cat 2 for hydrogen and comonomer. One explanation for the observed end group selectivity and sensitivity to the chain transfer agents could be the dominance of different termination mechanisms. Alternatively, the tetrahydroindenyl ligand may promote a higher steric barrier toward the active center, owing to its less rigid ligand structure.[25] This would slow the propagation step (the polymerization activity alone does not reveal this because the number of actual active centers is unknown). The slower the propagation step, the more probable it is that the growing chain undergoes a recoordination step.[28] This recoordination route is likely to prevent[29] the insertion of a new monomer and leads to the formation of transvinyl end groups.[30-32] Furthermore, the use of hydrogen or comonomer would have a greater influence on the molecular weight because there would be more time for a chain transfer agent to take part in the chain growth process.

The different ability of the catalysts to produce vinyl ends in the polymer suggests that the polymers may also differ in the frequency and structure of their long-chain branches. In a recent discussion of the chain structure of long-chain branched polymers produced by single site catalysts, Zhu et al.[33] proposed that the long-chain branched polymers assume either dendritic or comblike structure, where the dendritic chain structure is a result of incorporation of branched macromonomers.

The Cat 1 polymers exhibited a high content of vinyl ends, very high complex viscosity at the lowest frequencies and high flow activation energy. These properties could result from a complex, dendritic structure in which the long branches are further branched. The rheological behavior of the Cat 1 homopolymers of highest molecular weight, which were produced at the lowest ethene pressures, even resembled that of cross-linked polymers in the very early stages of cross-linking. In our polymers, however, a branched, dendritic structure should be more likely than a structure with cross-links. The Cat 2 polymers, with their low content of vinyl ends, simpler dynamic rheological properties and only slightly elevated flow activation energy E_a, would more likely bear long-chain branches fewer in number and more linear than in the Cat 1 polymers.

Conclusions

The dynamic rheological behavior of the polymers produced with both catalysts suggests the presence of long-chain branches. The complex viscosities of the experimental polymers were higher and the frequency dependency was different from what one would expect for a linear polymer on the basis of the GPC molecular weight and rather narrow MWD. The polymers produced with $Et[Ind]_2ZrCl_2$/MAO had an Arrhenius-type flow activation energy of 50–60 kJ/mol, while the polymers produced with $Et[IndH_4]_2ZrCl_2$/MAO had a somewhat lower activation energy of 40 kJ/mol. Branches longer than six carbon atoms were detected in $Et[Ind]_2ZrCl_2$/MAO polymerized homopolyethene by ^{13}C NMR. The rheological properties of the polymers were influenced by hydrogen, monomer pressure, and the amount of comonomer.

End group analysis showed that both catalysts were able to produce vinyl-terminated polymer molecules but that $Et[Ind]_2ZrCl_2$/MAO was more selective than $Et[IndH_4]ZrCl_2$/MAO toward terminal vinyl unsaturation. Comonomer and hydrogen had more influence on the end group pattern with $Et[IndH_4]_2ZrCl_2$/MAO.

The rheological behavior observed is suggested to arise from the in situ incorporation of macromonomers in polymerization. We intend to investigate these findings further by studying the influence of polymerization parameters with other metallocene catalysts, to gain a deeper understanding of the incorporation of macromolecules.

References and Notes

(1) (a) Mehta, A. S.; Speed, C. S.; Canich, J. A. N.; Baron, N.; Folie, B. J.; Sugawara, M.; Watanabe, A.; Welborn, H. C. Exxon Chemicals, Int. patent WO 96/12744. (b) Lai, S. Y.; Wilson, J. R.; Knight, G. W.; Stevens, J. C.; Chum, P.-W. S. Dow Chemical Company, U.S. Patent 5,272,236. (c) Howard, P.; Maddox, P. J.; Partington, S. R. BP Chemicals Ltd., EP 0 676 421 A1.

(2) Shiono, T.; Moriki, Y.; Soga, K. *Macromol. Symp.* **1995**, *97*, 161–167.

(3) Carella, J. M. *Macromolecules* **1996**, *29*, 8280–8281.

(4) Vega, J. F.; Muñoz-Escalona, A.; Santamaría, A.; Muñoz, M. E.; Lafuente, P. *Macromolecules* **1996**, *29*, 960–965.

(5) (a) Hamielec, A. E.; Soares, J. B. P. *SPO'96* 95–115. (b) Hamielec, A. E.; Soares, J. B. P. *Prog. Polym. Sci.* **1996**, *21*, 651–706. (c) Beigzadeh, D.; Soares, J. B. P.; Hamielec, A. E. *Polym. React. Eng.* **1997**, *5* (3), 141–180.

(6) Sugawara, M. *SPO '94*, 39–50.

(7) (a) Haslam, J.; Willis, H. A.; Squirrel, D. C. M. In *Identification and Analysis of Plastics*, 2nd ed.; Iliffe Books: London, 1972. (b) Randall, J. C. *J. Macromol. Sci., Rev. Macromol. Chem. Phys.* **1989**, *C29*, 201–317.

(8) (a) Mavridis, H.; Shroff, R. *J. Appl. Polym. Sci.* **1993**, *49*, 299–318. (b) Mavridis, H.; Shroff, R. *J. Appl. Polym. Sci.* **1995**, *57*, 1605–1626. (c) Shroff, R.; Prasad, A.; Lee, C. *J. Polym. Sci., Part B* **1996**, *34*, 2317–2333.

(9) Harrell, E. R.; Nakajima, N. *J. Appl. Polym. Sci.* **1984**, *29*, 995–1010.

(10) Rudin, A.; Pang, S. *J. Appl. Polym. Sci.* **1992**, *46*, 763–773.

(11) (a) Lachtermacher, M.; Rudin, A. *J. Appl. Polym. Sci.* **1996**, *59*, 1213–1221. (b) Lachtermacher, M.; Rudin, A. *J. Appl. Polym. Sci.* **1995**, *58*, 2077–2094. (c) Lachtermacher, M.; Rudin, A. *J. Appl. Polym. Sci.* **1995**, *58*, 2433–2449.

(12) Carella, J. M.; Gotro, J. T.; Graessley, W. W. *Macromolecules* **1986**, *19*, 659–667.

(13) Bersted, B. H. *J. Appl. Polym. Sci.* **1985**, *30*, 3751–3765.

(14) Wasserman, S. H.; Graessley, W. W. *Polym. Eng. Sci.* **1996**, *36*, 852–861.

(15) Graessley, W. W.; Raju, V. R. *J. Polym. Sci., Polym. Symp.* **1984**, *71*, 77.

(16) Raju, V. R.; Smith, G. G.; Marin, G.; Knox, J. R.; Graessley, W. W. *J. Polym. Sci.* **1979**, *17*, 1183–1193.

(17) Kim, Y. S.; Chung, C. I.; Lai, S. Y.; Hyun, K. S. *J. Appl. Polym. Sci.* **1996**, *59*, 125–137.

(18) Zweifel, H.; Moss, S. *Polym. Degrad. Stab.* **1989**, *25*, 217–245.

(19) Foster, G. N.; Wassermann, S. H.; Yacka, D. J. *Angew. Macromol. Chem.* **1997**, *252*, 11–32.

(20) Brintzinger, H.-H.; Fischer, D.; Mülhaupt, R.; Rieger, B.; Waymouth, R. M. *Angew. Chem., Int. Ed. Engl.* **1995**, *34*, 1143–1170.

(21) Woo, T. K.; Fan, L.; Ziegler, T. *Organometallics* **1994**, *13*, 2252–2261.

(22) Siedle, A. R.; Lamanna, W. M.; Newmark, R. A.; Stevens, J.; Richardson, D. E.; Ryan, M. *Makromol. Chem. Makromol. Symp.* **1993**, *66*, 215–224.

(23) Tsutsui, T.; Kashiwa, N.; Mizuno, A. *Makromol. Chem. Rapid Commun.* **1990**, *11*, 565–570.

(24) Carvill, A.; Tritto, I.; Locatelli, P.; Sacchi, M. C. *Macromolecules* **1997**, *30*, 7056–7062.
(25) Lehmus, P.; Härkki, O.; Leino, R.; Luttikhedde, H. J. G.; Näsman, J. H.; Seppälä, J. V. *Macromol. Chem. Phys.* **1998**, *199*, 1965–1972.
(26) Leino, R.; Luttikhedde, H. J. G.; Lehmus, P.; Wilén, C.-E.; Sjöholm, R.; Lehtonen, A.; Seppälä, J. V.; Näsman, J. H. *Macromolecules* **1997**, *30*, 3477–3483.
(27) Spaleck, W.; Küber, F.; Winter, A.; Rohrmann, J.; Bachmann, B.; Antberg, M.; Dolle, V.; Paulus, E. F. *Organometallics* **1994**, *13*, 954–963.
(28) Busico, V.; Cipullo, R. *Metallocenes '96* **1996**, 323–333.
(29) Busico, V.; Cipullo, R.; Chadwick, J. C.; Modder, J. F.; Sudmeijer, O. *Macromolecules* **1994**, *27*, 7538–7543.
(30) Thorshaug, K.; Rytter, E.; Ystenes, M. *Macromol. Rapid Commun.* **1997**, *18*, 715–722.
(31) Babu, G.; Newmark, R. A.; Chien, J. C. W. *Macromolecules* **1994**, *27*, 3383–3388.
(32) Prosenc, H.-M., Brintzinger, H.-H. *Organometallics* **1997**, *16*, 3889–3894.
(33) Zhu, S., Li, D. *Macromol. Theory Simul.* **1997**, *6*, 793–803.

MA980522N